

**2019 NDIA GROUND VEHICLE SYSTEMS ENGINEERING AND TECHNOLOGY
SYMPOSIUM
MODELING & SIMULATIONS, TEST & VALIDATION (MSTV) TECHNICAL SESSION
AUGUST 13-15, 2019 - NOVI, MICHIGAN**

**MATURATION AND TRANSITION OF
ENERGY ABSORBING DAMPERS**

J. Mathis¹, M. Grimm¹, S. Mullin¹, V. Burgess²

¹Engineering Dynamics Department, Southwest Research Institute, San Antonio, TX

²U.S. Army Combat Capabilities Development Command Ground Vehicle Systems
Center, Warren, MI

ABSTRACT

Southwest Research Institute® (SwRI®), under contract to US Army CCDC-GVSC, went through an extensive design, analysis, manufacturing, and testing project for the development of energy absorbing dampers and lightweight floor systems to provide protection to the warfighter inside vehicles that are exposed to underbelly blasts or similar threats. The dampers have been designed to remain locked during a wide variety of road vibration and shock loads, but to release and absorb energy through elongation, providing protection to occupants when the blast threats are encountered. This range of input criteria was challenging to satisfy in a passive system that is lightweight, relatively inexpensive, easy to install, and effective over a wide range of blast loads and occupant weights (5% through 95%). The SwRI work concentrated on designing two subsystem sizes – the individual dampers themselves in component tests, and ½ scale coupon level tests that include the dampers, floor systems, and attachment hardware. Working directly with SwRI, CCDC-GVSC integrated component level damper designs into full vehicle scale test articles. Full-scale vibration and durability testing was conducted at CCDC-GVSC's PS&T facilities on their MEVT test fixture and subsequent live fire blast testing. These test programs and the results achieved are described in the paper.

Citation: J. Mathis, M. Grimm, S. Mullin, V. Burgess “Maturation and Transition of Energy Absorbing Dampers”, In *Proceedings of the Ground Vehicle Systems Engineering and Technology Symposium (GVSETS)*, NDIA, Novi, MI, Aug. 13-15, 2019.

1. INTRODUCTION

Southwest Research Institute, under contract to CCDC-GVSC, has been developing energy absorbing (EA) dampers and lightweight floor systems to provide protection to the warfighter inside vehicles that are exposed to underbelly blasts or similar threats. The floor system is suspended by EA dampers that are designed to stroke independently of the hull, as it is blasted upwards, thus reducing the loading into the legs. The

dampers represent a passive system that is lightweight, relatively inexpensive, easy to install, and effective over a wide range of blast loads and occupant weights (5% through 95%). In the early phases of this project, the basic designs were created and their capability demonstrated through drop tower and small-scale blast tests. Figure 1 illustrates the general geometry of the damper in normal and stroked conditions.

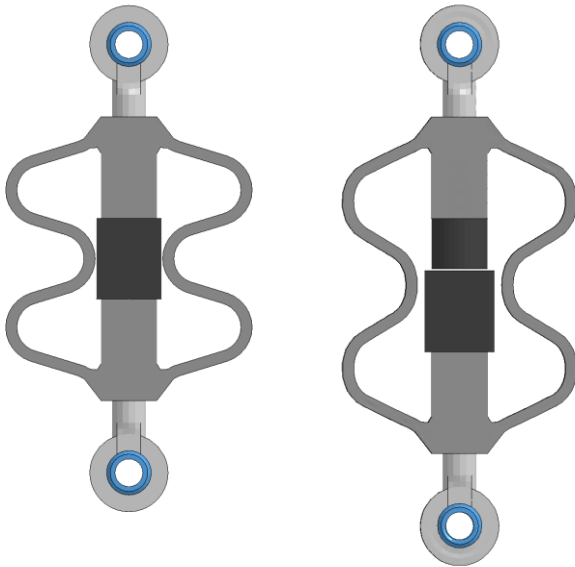
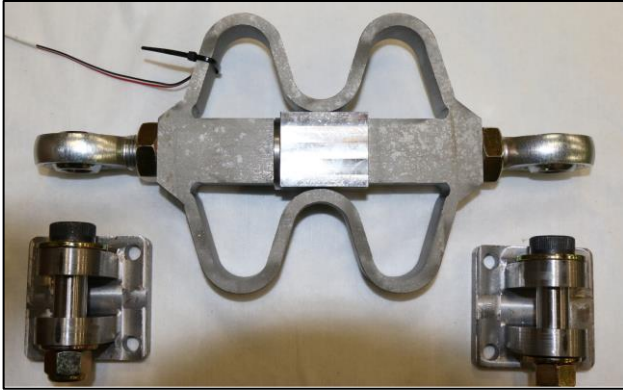


Figure 1: EA damper in normal (left) and stroked condition (right).

The most recent phase of this work has focused upon maturing the design and subjecting it to a series of durability tests that mimic worst-case shock loads and road vibration loads. To withstand the road shock and vibration, it was necessary to incorporate a breakaway device into the damper design. Research was conducted on many options for this purpose. Some of the work focused upon COTS systems and others on novel designs, keeping focused upon project goals of simplicity, low cost, and easy maintenance. The designs we investigated included two COTS options: tensile screws and interference clips were evaluated and

are described herein. CCDC-GVSC expressed concern about the tensile screw design, based on other previous work that indicated potential unreliable operation. To ensure the consistency of performance when materials are sourced from several vendors and machining operations are required, SwRI conducted a focused quality assurance task on these screws, running many repeat tests on a variety of sourced hardware. Results indicated the processes were sound, and the bounds upon performance in terms of breaking load were established.

To evaluate performance under road, road shock, and blast loading, extensive simulations and testing were performed. The process used in the finite element calculations for dynamic loading and fatigue are described and compared to the experimental results. Test fixtures were built to support single dampers (component tests) and sections of the floor with four dampers (coupon tests). These were subjected to testing on an electrodynamic shaker table, shock testers, drop towers, and blast tests. Some design options failed during this sequence of tests; the approach used and lessons learned from that exercise is described. The interference clip design passed the fatigue testing, but in subsequent shock testing, was noted to have issues with fatigue-induced galling. The tensile screw design was revisited, and a hollow version was devised that passed all required tests. A wealth of experimental data was obtained in the testing; highlights are provided in this paper.

2. DURABILITY REQUIREMENTS

In order for the EA floor system to be practical inside a combat vehicle, the system should be able to withstand regular use, defined as a set of operational conditions that the vehicle may be subjected to over a defined period of time/cycles or miles. Considerations include static occupant loads, as well as dynamic loads from mounting/dismounting. Of far greater concern are the loads that the floor system is subjected to during vehicle operations. Operation loads can be broken

down and quantified as road shock loads and vibration loads. Road shock loads may be generated by collision with obstacles or suspension response to large bumps that are encountered at high-speed. Vibration loads are more difficult to quantify because they are random in nature and occur continuously during operation but vary based on speed and terrain. CCDC-GVSC has a vast amount of data from vehicle proving test programs and provided the representative road shock and vibration loads to SwRI for this program. Since this flooring application was designed for a concept vehicle, the road shock and vibration load data was synthesized from simulations. Figure 2 shows the vibration spectrum loads that were used for our analysis and testing. The road shock loads consisted of 12g-35ms half-sine pulses along the vertical axis and 5g-35ms half-sine pulses along the longitudinal and transverse axes.

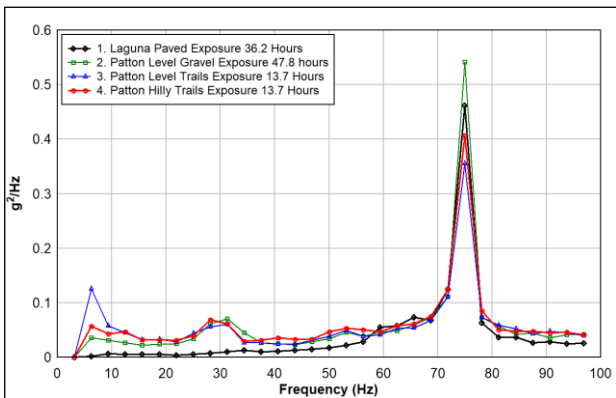


Figure 2: Vibration spectrum loads.

The EA mechanisms of the damper system alone are not designed to withstand the road shock and vibration loads. In fact, these mechanisms would fail from fatigue or deform plastically during regular operation. Therefore, part of the design of the EA was to incorporate a mechanical breakaway mechanism that was designed to hold the floor in position during road shock and vibration but release during an under-body blast event. In order to design the breakaway, forces encountered during road loads and blast loads needed to be quantified. Loads

were quantified using dynamic finite element simulations performed in LS-Dyna. The weight used on the floor was that for the 95-percentile occupant, to obtain the most conservative (largest) forces. These values are compared to similar calculations performed using the design blast inputs to determine the difference in peak force magnitudes between the events. Figure 3 shows the result of this calculation and shows the finite element model of the floor system used for this analysis.

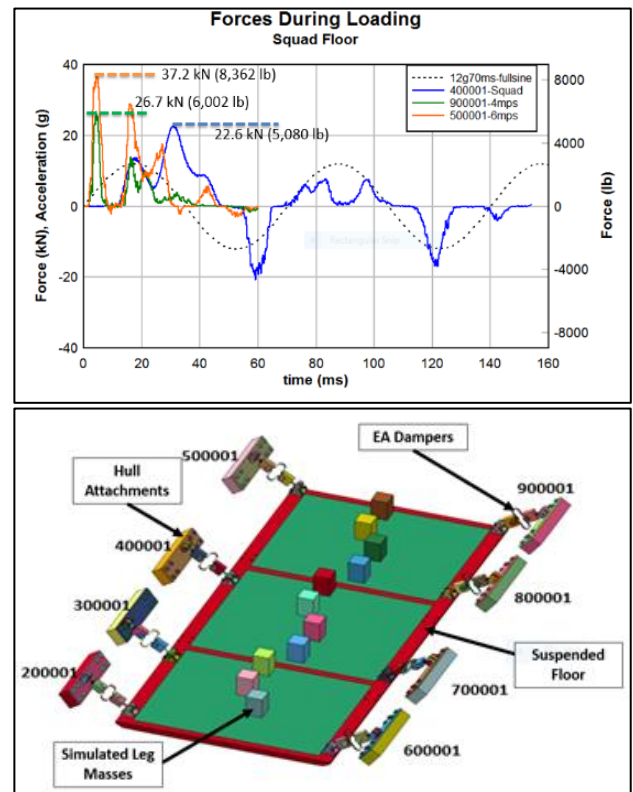


Figure 3: Forces quantified (top) using FEA simulation models (bottom).

Note that the data shown in Figure 3 represents the maximum force calculated over the eight attachment locations. It can also be seen that there is not a large spread between the peak forces occurring during road shock (5,080lbs.) and the minimum blast level force (6,002lbs.) for the lower level blast input. This means the design for the breakaway device needs to be very precise if it is to

hold during the worst-case road shock event but open during the lower level blast event. The following sections describe some of the various breakaway options that were identified as having potential and the results of baseline tests with some of those options.

3. BREAKAWAY TECHNOLOGIES

3.1. Belleville Washer Force Limiter

A vendor with a COTS solution to a force limiter capable of generating forces required to resist the road shock loads and release at higher loads was identified. The vendor was Ringspann GmbH, and their product is a customizable force limiter based on stacks of Belleville washers, as shown in Figure 4. The devices can readily supply the forces required and release rapidly once a pre-determined force is applied. A conceptual design of the EA damper that includes the integral Ringspann device is also shown in Figure 4.

3.2. DCD Pins

SwRI identified a vendor with a COTS solution that is similar to the tensile screw design, which was of interest to CCDC-GVSC, since it was a commercially available, vetted alternative, shown in Figure 4. The pins are designed to break at a precise load, and there are up to five of them located in a holder mechanism. The device can handle break forces from 750lbs. to 12,500lbs., depending on pin combination used. A special 3-part connector design limits moment/bending on the pins and has integral end clevis for simplified connection. The COTS pin holder did not fit the damper design, so a custom pin holder was required. The custom pin set cartridge was designed to accept the OEM DCD fracture pins in a configuration similar to the OEM breakaway connector, while integrating into the current EA damper design. This custom design is also shown in Figure 4.

3.3. Tensile Screws

It was desired to include the breakaway device integral to the EA to simplify the overall design and make maintenance easier. A concept that used a single tensile screw in the center portion of the damper is shown in Figure 4. The basic operating principle of the tensile screw is to weaken it such that it will break abruptly over a narrow range of force. The screw is contained in a cartridge such that the bottom part is affixed to the lower EA damper, and the top part is connected to the upper EA damper portion. The cartridge is made of concentric steel sleeves that provide lateral support and bending resistance, so the force is directed axially through the screw. The concentric rings are in close contact but not connected, so that when the tensile screw breaks, the damper is free to extend and absorb energy. FEA simulations were conducted to confirm the operation of the assembly and to design the screw notch diameter to operate properly under the loading conditions described later in this paper.

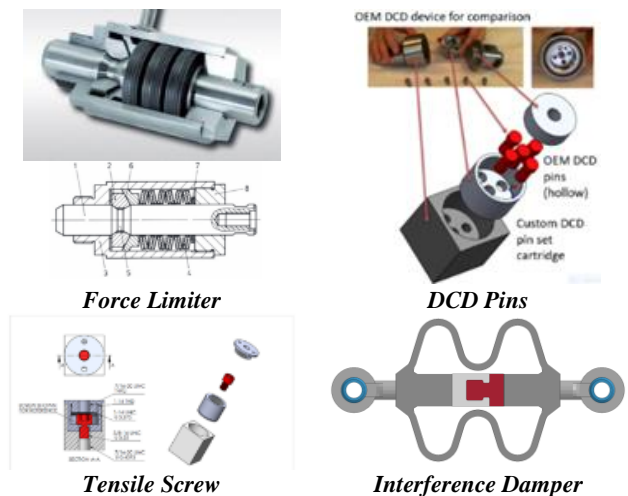


Figure 4: Breakaway technologies.

3.4. Interference Damper

SwRI devised an alternative breakaway mechanism that relied upon the plastic bending of two linked pieces or clips. This device was called the “interference damper”. The concept was to have the linked pieces be independent of each other but

in close proximity, essentially a zero clearance fit. Since the load path through the damper would run through the breakaway device, close proximity is required to minimize the effects of the repetitive impact loads due to the road load vibration spectrum. When the blast event creates a tensile load exerted on the damper ends the load would be sufficient to bend and separate the clips, allowing the force to be carried through the EA portion of the damper. The interference damper device is shown in Figure 4.

4. TECHNOLOGY DOWN-SELECT

Three breakaway designs were selected for detailed analysis, refinements, and a full spectrum of component level tests. The tensile screw, DCD pins, and interference damper were selected based on metrics of performance, space claim, cost, and manufacturability. Through detailed analysis and later confirmation through testing, all three technologies were proven sufficiently robust to resist the road shock loads, and it became clear early on that fatigue loading would be the driver for the designs. The entire EA system, which includes the EA damper, breakaway device, rod ends, upper and lower clevis (lugs), and shoulder bolts needs to withstand the road load spectrum discussed earlier. Depending on the technology, different analysis techniques were used to estimate fatigue life.

5. TENSILE SCREW DESIGN

The tensile screw design focused on selection of the appropriate notch diameter that would not yield during road shock loads but would quickly break during the lower level blast load case. The design would also need to be resistant to the full fatigue load spectrum. Early on in the tensile screw design phase there were concerns about variability in material strength within the same ASTM A574 (UTS = 170,000psi, yield strength = 150,000 psi) specifications, depending on the manufacturer of the screw. In addition, there were concerns with the surface quality of the machined notch. Five manufacturers of ASTM A574 screws were

selected, and five notched specimens from each manufacturer were machined then tensile tested. The results indicated that differences in breaking force as a function of notch surface quality and screw manufacturer were considered small and within reasonable tolerances for our application, (deviation from average break force was approximately 1%). Thus, any of the manufacturers would suffice, and the machining operation was of sufficient precision to produce repeatable results with respect to the desired breaking load.

A simple $\sigma=F/A$ model for predicting tensile screw fracture force is not accurate for a notched specimen due to the stress triaxiality and notch strengthening effects. Therefore, the notch diameter was selected using FEA simulations that required an accurate material model for the screw. Tensile tests were conducted on notched Grade 8 bolts by SwRI for another CCDC-GVSC program to fully characterize the material. The improved modeling approach was applied toward this program in design of the notch for the screw. In parallel, a finite element mesh sensitivity study was performed to quantify effects of element size on the predicted results.

The design of the tensile screw breakaway integral to the EA Damper requires a short (3/8 inch x 1/2 inch length) screw. A series of simulations were conducted using the validated ASTM A574 bolt model to determine the notch diameter that achieved the desired breakaway force. An empirical model was generated based on the fracture force and notch diameter using the simulation results, shown in Figure 5. The model is non-linear due to notch strengthening effects. A notch diameter of 0.156-inches is predicted to achieve the target fracture force of 5,500 lbf. This prediction was validated with the breakaway experimental tensile test series, discussed next.

Before component durability tests were conducted on the full damper system, the tensile screw breakaway device by itself was fabricated and tested in tensile pull tests to ensure that the proper breaking force would be achieved. The bolts

used were obtained from Holo-Krome: 3/8-24 x 1/2 socket head cap screw ASME B18.3 ASTM A574. Seven of these screws cut with the 0.156-inch diameter notch were tested with good repeatable results. Detailed fatigue and preload analysis was performed and is discussed in a later section in this paper.

SwRI designed a version of the DCD pin breakaway device to hold them in a manner similar to the tensile screw. The appropriate pins were selected and tested for the 5,500lbs. break force based on manufacturer's recommendation, and therefore no detailed analysis was performed for the DCD solution.

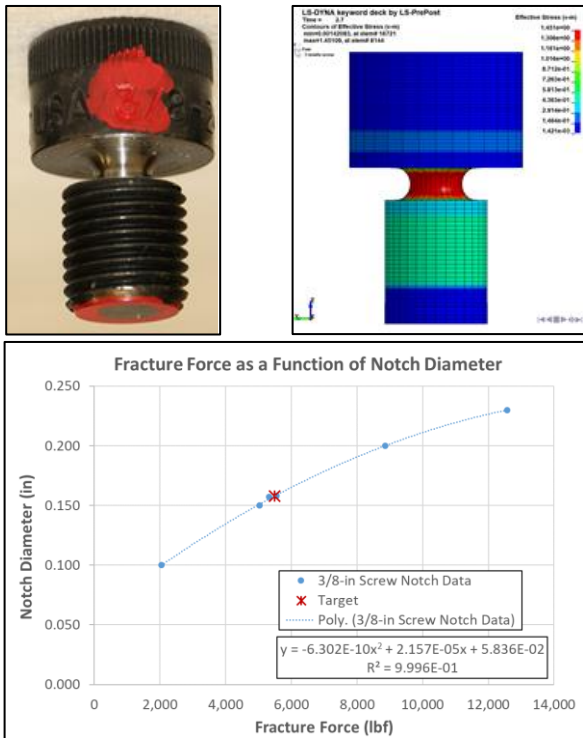


Figure 5: Validated FEA simulations to develop empirical model for failure force vs notch diameter.

6. INTERFERENCE DAMPER DESIGN

The interference dampers were designed with the use of FEA simulations that predicted the opening force required for the different clip geometries, as shown in Figure 6. All interference breakaway designs used the same 304 SS material as in the

other portions of the damper. The design operates in the regime of plastic deformation but not material failure. Forces can be altered by adding or removing material in critical areas, so the concept is very scalable. The design can also be tailored to how much deflection occurs before full release.

To determine fatigue life, S-N curves for metals used in the design were 304 SS for interference dampers, 6061-T6 for the floor, and 4340 steel for the other hardware and parts. LS-Dyna was used to perform a fatigue analysis of the damper and connection hardware. The random vibration fatigue analysis used excitation inputs from Figure 2 and calculated the root-mean-square (RMS) stress in the clip region. Predicted RMS stress was approximately 20% of the material ultimate tensile strength.

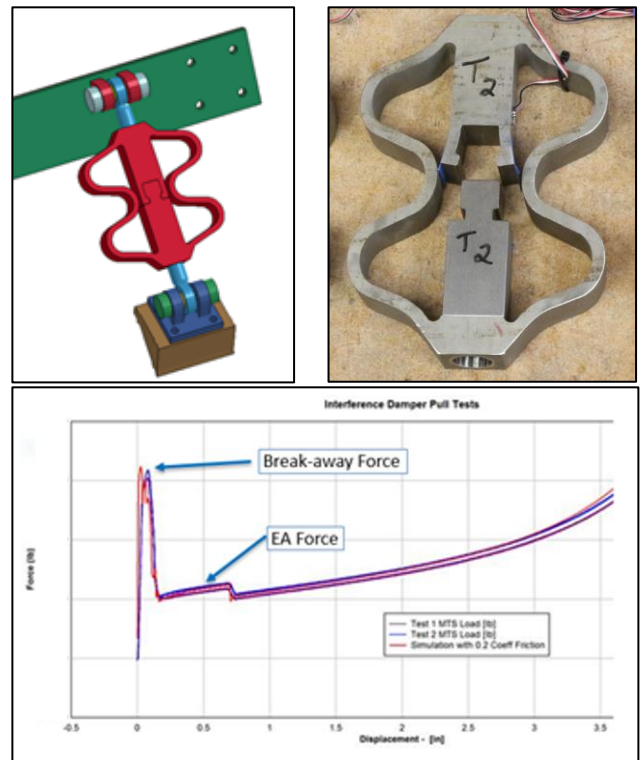


Figure 6: Interference damper FEA model, fabricated assembly, and analysis results compared to test.

Considering that the design for fatigue resistance would generally require stresses below 20% of material yield, the analysis showed that the design

would certainly not have infinite life and failure may be expected at some number of cycles, however, the fidelity of the analysis did not allow precise prediction. Through several analysis iterations, it was found that small geometry changes, clearances, contact algorithms, initial stresses, and friction all played key roles in influencing the results of the analysis. Certain combinations of the aforementioned variables did suggest better performance than the initial analysis results indicated. The appropriate action in this case was to move forward with fatigue tests in order to generate data that could be used to validate analysis techniques and in parallel prove the design.

7. COMPONENT TEST METHODOLOGY

The goal of the component testing is to subject a single EA damper and breakaway assembly to the various input loads under realistic conditions including road shock, simulated blast (drop), and fatigue. The basic assumption for all the damper design work is that the vehicle hull is “rigid” – this condition was replicated in the component test fixture by attaching the upper end of the damper to a very stiff structural member. The other important condition to replicate was the allowance for free vertical motion of a representative floor mass. The approach used to accomplish this was to attach the lower end of the damper to a weighted structure that translated vertically on bearings to simulate the boundary conditions of the floor. This approach can be seen in the test setups shown in Figure 7 and Figure 8. The “floor” member was a steel box where weights could be placed to mimic different floor masses. The mass box was weighted to 70lbs. to represent the most weight carried by any single damper (included floor mass and occupant leg mass). The clevis on the lower end of the damper was bolted into an aluminum 6061-T6 block that was bolted to the steel mass box. The other side of the steel box was bolted to a flat plate that attached to the bearings that rode on the vertical shafts. The remainder of the fixture was constructed of structural steel.

8. COMPONENT ROAD SHOCK TESTS

Each integral breakaway damper design was subjected to the road shock test profiles using the MTS drop table calibrated to produce the 12g-35ms half-sine shock pulse, as specified by CCDC-GVSC. The tests were instrumented with strain gauges on the EA dampers, accelerometers for measuring input and response, and a custom load cell integral to the upper rod end to measure axial forces in the EA. All three EA designs passed the 18 repeated drops for the road shock tests. Typical data from these tests exhibited peak dynamic forces of approximately 3,000lbs.

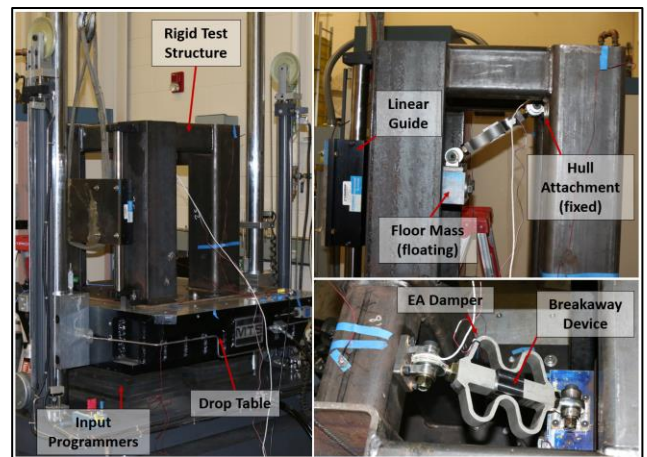


Figure 7: Component level test fixture.

9. COMPONENT FATIGUE TESTS

The vibration load spectrum defined by CCDC-GVSC was provided to the component test fixture using an Unholtz-Dickie Model SA30E-T1000IAR-64 shaker that provides a broad frequency excitation. This machine is shown in Figure 8 with the component test fixture installed. This machine provided all of the vibration spectrum input loads, as described subsequently.

The vibration-testing machine is driven using the PSD input (Figure 2). The PSD profiles are run continuously to cover the time of interest, which according to the 5000-mile OPTEMPO operational requirement would be 111.4 hours of duration broken down into four terrain profiles.



Figure 8: Electrodynamic shaker used to provide road vibration loads.

SwRI personnel would monitor the vibration tests as they occurred, and between the 4 different cycles, would pause the testing to carefully examine the fixture and the damper assembly components to observe and document the results. Fatigue tests began with the interference damper; the design that analytical predictions say has the best chance to complete the whole sequence. Following the interference damper, testing was done on the tensile screw and DCD pin assembly. Table 1 summarizes the results of the fatigue testing.

10. FATIGUE TEST RESULTS

Some key observations were made during the fatigue testing campaigns. The initial rod ends selected were not adequate and were upgraded during the fatigue test campaign. Shoulder bolts connecting the rod ends to the upper and lower clevis (lugs) exhibited moderate wear, and for further tests, were installed with lubrication. Some hairline cracks appeared in the mounting clevis (lugs) resulting in a redesign. It was also observed that on fatigue tests where the breakaway device failed, the EA damper also quickly failed.

As is shown in Table 1, the notched tensile screw and DCD pin assemblies failed the fatigue campaign at 107.7 hours (97%) and 52.6 hours

(52%), respectively. The considerably lower fatigue life of the DCD pin system can most likely be attributed to the fracture pin's aluminum construction and more severe stress concentrations at the upper and lower portions of the gauge sections.

Table 1: Summary of fatigue testing.

<p><i>Interference Damper – Passed 111.4 Hours (100%)</i></p>		
<p><i>Notched Tensile Screw – Failed at 107.7 Hours (97%)</i></p>		
<p><i>DCD Pin Assembly – Failed at 52.6 Hours (52%)</i></p>		

The interference damper successfully completed the entire fatigue campaign with no signs of elongation or cracking in the clip release section. However, drop tests on the post-fatigued unit revealed that the damper was seized and would not stroke under blast loading conditions. Post-mortem analysis of the unit revealed fatigue induced wear (commonly referred to as galling) at the contact surfaces of the clip release mechanism. This galling was suspected to have added additional friction between the contact surfaces, ultimately preventing the clips from releasing and allowing the damper to stroke. The fatigue campaign was repeated with a second interference damper equipped with a harder nitronic steel clip section in hopes to mitigate galling at the contact surfaces. This damper also passed the fatigue campaign, but regrettably suffered the same post-fatigue seizure during blast loading. A final modification was made to a third interference damper, which involved adding

lubrication to reduce friction and wear between the contact surfaces. Unfortunately, the addition of lubrication promoted more relative motion between the contact surfaces of the clip mechanism and an increase in cyclic bending stresses. This caused the interference damper to fail during the fatigue campaign.

11. EVOLUTION OF THE TENSILE SCREW

Due to the complexities associated with the interference damper design and risk involved with testing modified designs with special coatings, etc., it was decided to go back to our second best performer determined from the component testing, which was the tensile screw design that passed though 97% of the fatigue campaign. Leveraging the wealth of test data and material models generated during the previous investigation, it was believed that slight modifications to the design could yield a passing result in fatigue.

Due to stress concentrations encountered with the notched design, the tensile screw was changed to a hollow core design. FEA simulations using previously developed material models and analytical techniques were used to size the inner diameter of the hole through the screw at 0.250-inches. The ID was precision honed to an 8 μ -inch finish, as shown in Figure 9.



Figure 9: Hollow tensile screw design.

Preload and fatigue analysis were repeated for this design, along with preload vs. torque tests. Using this data, a preload diagram shown in Figure 10 was used to assess the joint due to preload uncertainty. At the lowest possible preload levels, there was risk that the joint could open under peak loads, which would increase stresses in the screw substantially. However, increasing the nominal preload any more

would jeopardize the screw by operating near the yield at the upper end of the preload spread.

To determine how the preload could affect fatigue performance, a Goodman analysis was performed, as shown in Figure 11. At the RMS and 3- σ RMS load level, all points regardless of preload fall below the Goodman line, indicating essentially infinite life. However, points do fall above the Goodman line for peak loads, regardless of preload, indicating finite life at peak loads. Using the S-N curve for the screw material, a life of approximately 125,000 cycles was predicted at peak force levels. Fortunately, based on available test data from the component fatigue testing, peak loads are not encountered frequently, and in fact, were estimated from test data to occur less than 10,000 times, only during the most severe of the fatigue PSD profiles.

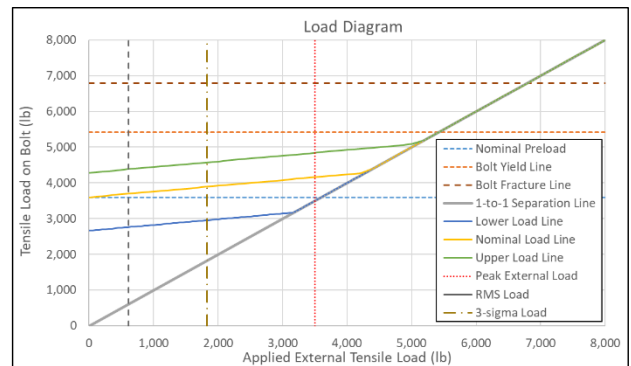


Figure 10: Screw preload diagram.

After the hollow tensile screw had been fully vetted for preload and fatigue, several tensile pull tests were conducted yielding an average breakaway force of 7,050lbs. Fatigue testing was conducted next to confirm the design at component level. The result was a success with the assembly passing the entire fatigue campaign. A component level drop test was then conducted using the post-fatigue tensile screw to simulate a medium level blast load. During that test, the breakaway operated as designed, and the floor mass stroked 1.37-inches. The rod end load cell measured peak a breakaway force of 7,869lbs. and a constant EA force of 2,585lbs. This was a confirmation that the

component hollow tensile screw EA was working as designed, completely passing fatigue and operating under blast load.

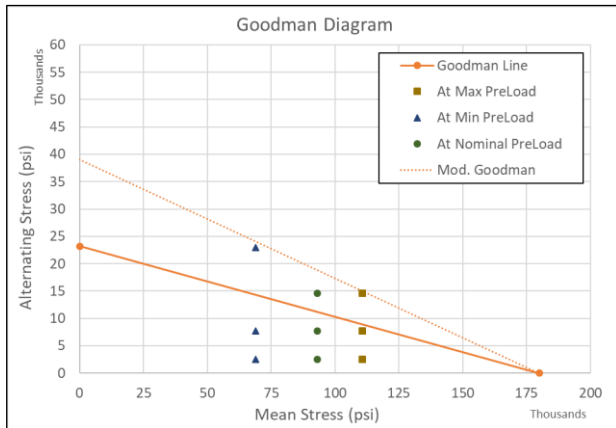


Figure 11: Goodman fatigue diagram.

12. COUPON FATIGUE TESTS

Coupon level fatigue tests were next conducted using the hollow screw design. This used the coupon fixture shown in Figure 12 that had four of the damper assemblies and an appropriated weighted 1/3-length floor section. Two of the four EA's had a load cell integrated into the upper rod end, and accelerometers were used to monitor the response of the floor and fixture due to the input PSD. This test was again system-level and incorporated design revisions for the transverse panel interface with the hull using a polyurethane bushing and washer assembly. The bushing assembly is designed to resist transverse and longitudinal road shock pulses but allow the floor to freely stroke vertically during a blast. Transverse and longitudinal shock testing was not in the scope of this program but rather was assessed through FEA simulations.

During initial startup of the coupon fatigue test, it was noticed that loads at one of the monitored EA's was significantly above what was observed in the component tests, but the cause was initially unknown. Further investigation indicated that the mass ballast plate in the center of the floor was exhibiting some resonance, which was driving

higher than expected loads into the floor. This excessive loading was believed to be what contributed to a failure of one of the tensile screws during this fatigue test that occurred late in the first PSD profile. This was not a consistent result when compared to the component level tests. It was determined that the ballast mass should be more realistically attached to the floor, as its purpose is intended to represent the mass of the occupants legs on the floor. A blast mat was installed, and simulated foot contact areas under the ballast plate were added. Load cells were added at all corners to monitor forces and ensure the static load was balanced properly during the setup, which was not done during the first test series. Incorporating these changes, the fatigue test was repeated. The result of the test was a complete pass with tensile screws and transverse panel bushing assemblies performing as expected with no failures, as show in Figure 12.

13. COUPON LIVE FIRE TESTS

The coupon test assembly was subjected to blast testing to validate its performance during a simulated under the under-body blast event. Two tests were conducted; the first test subjected the post-fatigue tested specimen to the blast, while the second test used all-new damper assemblies. The coupon assembly was attached to the SwRI reusable landmine test fixture, as shown in Figure 13. A composition C-4 charge was buried in an engineered soil pedestal and positioned under the test fixture, also shown in Figure 13. The charge weight and standoff was selected to replicate the medium-level blast input loading.

The setup was instrumented with load cells to measure the forces in each of the dampers, accelerometers to measure blast input to the fixture and floor response, and external high-speed video to measure total fixture jump height and initial velocity (impulse). In addition, two high-speed video cameras were mounted to the floor on-board the fixture to measure floor stroke at each damper location using a 2-D digital image correlation analysis technique.

MATURATION AND TRANSITION OF ENERGY ABSORBING DAMPERS

The floor system performed as designed during both blast test exposures. The tensile screws released and allowed the floor to stroke through elongation of the EA dampers. The transverse support panel and bushing assemblies, designed for transverse road loads, performed as designed by allowing the floor to release without binding and to stroke vertically with no interference. Figures 14 and Figure 15 show some of the data collected during the blast tests. The difference in the average floor stroke between the two tests was 0.1-inch, and breakaway forces and EA forces were very similar as well. Peak breakaway forces were higher for the blast test than what was observed for the component drop. This is believed to be a result of load-rate dependence, as the loading rate in the blast test was significantly higher than the drop testing. The increase in the breaking force did not affect the performance of the system as a whole.

The interference damper design had many positive characteristics, however; complex galling issues that arose during fatigue testing could not be completely resolved. As a result, the tensile screw design was matured and ultimately passed all fatigue testing. The virgin and fatigue-tested tensile screw damper was then blast tested and performed successfully, as designed.



Figure 12: Coupon level test fixture.

Breakaway designs for the EA damper were matured and tested to road shock, fatigue, drop, and



Figure 13: Blast test setup.

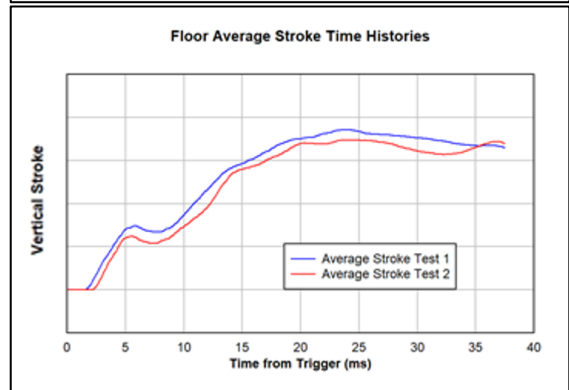
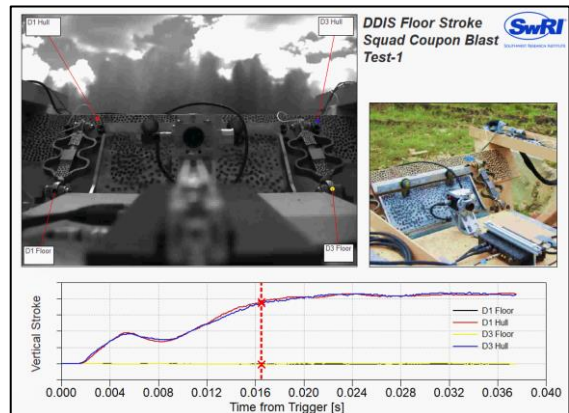


Figure 14: Dynamic floor stroke data.

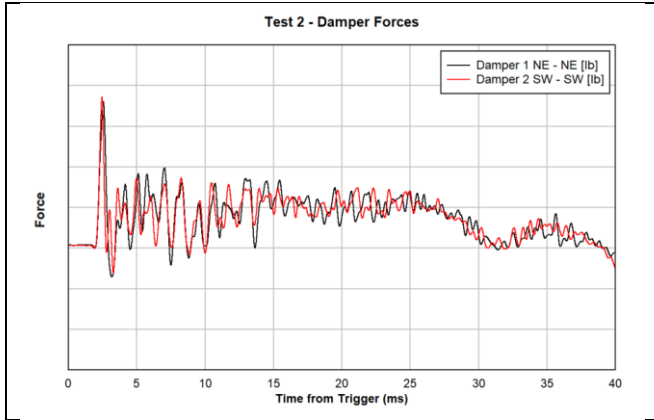


Figure 15: Damper force histories.

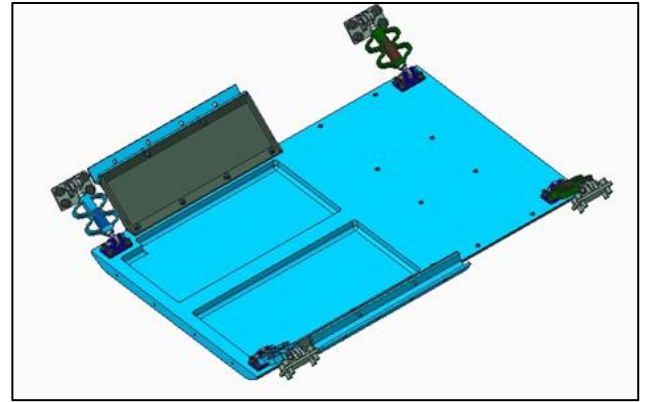


Figure 16: Crew floor configuration.

14. INTEGRATION INTO FULL SCALE VEHICLE SYSTEM

Leveraging the work performed by SwRI, CCDC-GVSC worked to integrate the stroking floor technology into a vehicle with other systems such as Hull and Seat technologies. For this effort, a reconfigurable asset-sized hull article was used for physical demonstration. The reconfigurable asset allows the use of a full width hull but is constrained to 96 inches in length. The asset can be configured for a full scale crew configuration or a full width and 2/3 length squad configuration.

The crew configuration consists of the Driver and Commander forward facing with the seats mounted directly to the floor. The floor without seats or blast mats is shown in Figure 16. The squad configuration consists of four squad members facing each other with the seats mounted to the hull lower wall. Only the weight of their legs rest on the floor. The squad floor without blast mats is shown in Figure 17.

For both designs, a pocket that is 1.5 inches deep is machined into the walking floor to accommodate a blast mat.

The squad configuration was integrated first. Since the seats and floor perform independently, this is the most complicated configuration. The floor model was placed in the assembly with the hull and seats. Figure 18 depicts an integrated seat, floor, and hull assembly.

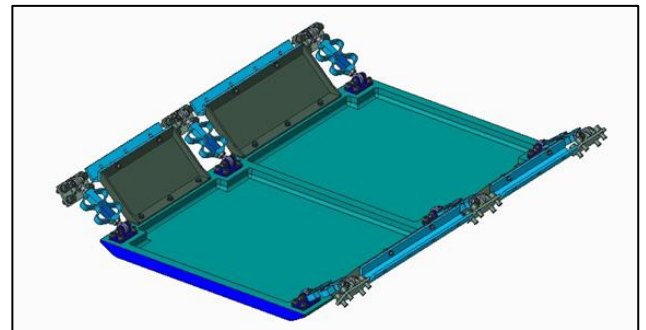


Figure 17: Squad floor configuration.

Since the seats stroke in a downward motion, the model needed to be checked in both the current ride height and the fully stroked position. Initially, the seat and the floor would impact each other when the seats fully stroke. Since the design of seat technology used for this effort is not adjustable, it was determined that if a change was made it would have to be in the floor design. Three potential options were developed. The first option was to leave the design as is. During a blast event the seat would only be able to stroke 4.1 inches of the 6.0 inch total before impacting the floor technology. Figure 19 shows option 1 with the seat fully stroked and the floor in its stroked position. It is observed that the lower part of the seat and the floor EA and transverse bracket impact each other.

Option 2 investigated dropping the floor EAs through a notch cut in the walking floor and mounting the EA on from the bottom. Figure 20 shows this design option looking down at the floor

with the notch cut out and the EA lowered by 2.0 inches. Option 2 increased the capable stroke of the seat to 5.25 inches of the 6.0 inches, however it required extensive modifications to the floor technology as well as the hull technology to move all of the mounting holes down.

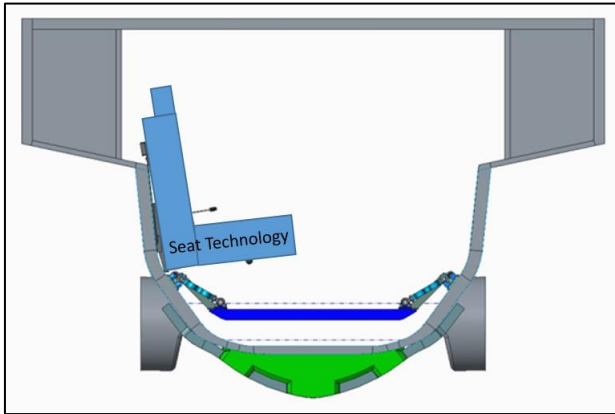


Figure 18: RA hull with floor and seat technologies.

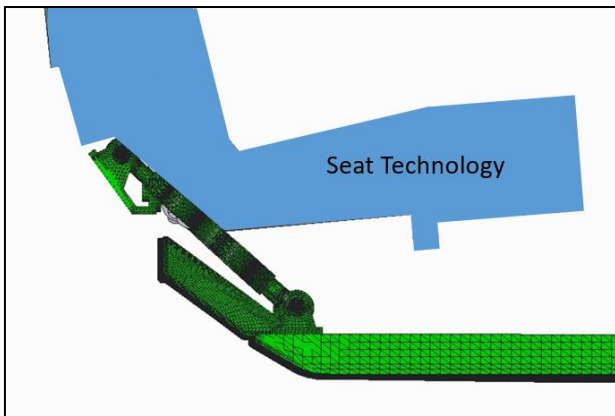


Figure 19: Floor and seat interference.

Option 3 extends the floor by 10.0 inches in length to allow for the EAs to be relocated in-between and outside of the seats. This option also lowered the transverse panels and shifted them inward in order to tuck them under the seats in their fully stroked position. Figure 21 shows a top view of Option 3 with all of the EAs clearing the seats. Option 3 required extensive modification to the floor and the hull technologies to move the mounting locations. Option 3 was determined to be the best option because it did not restrict the capable stroke of the

seat and there wasn't time in the seat development schedule to determine if the seats would require the full 6.0 inches. Option 3 also provided an advantage that the floor and seat would not impact each other even in the event that the seat fully stroked and the floor did not stroke at all. This option was then fully integrated into the CAD model and the drawing package was updated.

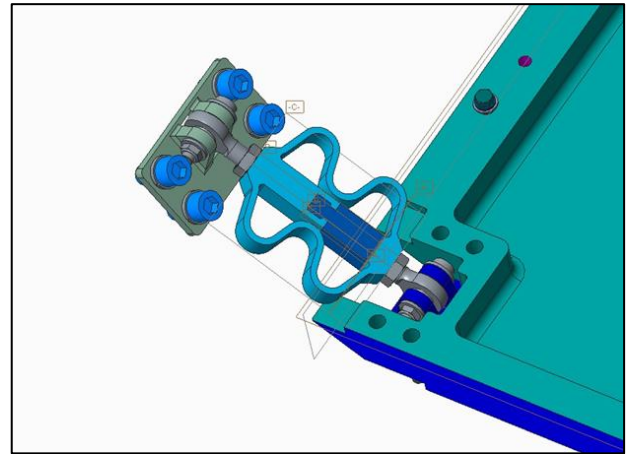


Figure 20: Option 2, bottom mount EA design.

The integration of the crew floor was more straightforward because the seats mount directly to the floor. The bolt patterns of the crew seats were verified and implemented onto the floor. Since adjustability was added to the seat, the seat can move both vertically and fore/aft. For the integration of the crew floor, the seat was checked in the two worst-case positions. First, positioned down and forward. Second, positioned down and backward. Since the crew seats mount along the edge of the floor on the sides, there is limited space for transverse panels. In order to keep both the crew and squad floors consistent, the option 3 transverse panels were implemented in the crew design as well. This low profile design allowed the transverse panels to extend farther back under the seat than previously. This provided additional lateral support for durability loads. Figure 22 shows the crew configuration with the transverse panel design from Option 3. The next step was to finalize the drawing

package for use in future testing with Option 3 fully integrated.

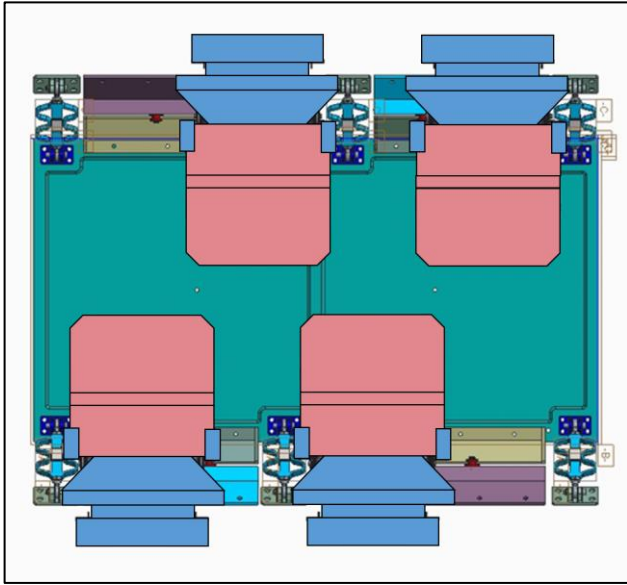


Figure 21: Option 3 with updated transverse panels.

15. DURABILITY LOAD CASES

The floor technology requirements call for two different load cases. The first is a road load durability case and the second is a shock input load case. The road load durability case used for this test series utilized actual accelerometer data taken from a Bradley Fighting Vehicle. This data was then compiled to create a 3000 mile load case over multiple terrains. The shock load cases were derived directly from the vehicle requirements. Since the floor design includes the crew and squad sections, different shock loads were determined based on the distance from the virtual center of gravity of the vehicle platform. The load cases used for the crew and squad configurations are shown in Table 2.

The next step was to work with CCDC-GVSC's Physical Simulation and Test (PS&T) group to determine the correct setup required to test each configuration because the test assets were sized for the reconfigurable asset. A test fixture was designed to accommodate both floors in all load cases. This effort was led by the PS&T team to

ensure proper fitment on their vibration tables, however it leveraged the current reconfigurable asset hull technology design to ensure proper integration of the floor technology. Figure 23 shows the floor fixture with the crew floor installed for reference.

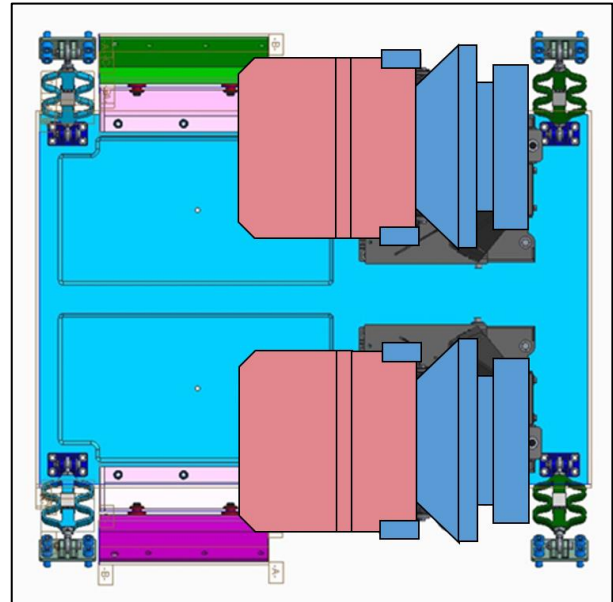


Figure 22: Crew floor with Option 3 designs implemented.

Table 2: Shock load cases.

Direction	Crew	Squad
Vertical	+/- 5g, 70ms sine pulse, 18 cycles	+/- 12g, 70ms sine pulse, 18 cycles
Horizontal (fore/aft and cross car)	+/- 5g, 70ms sine pulse, 18 cycles	+/- 5g, 70ms sine pulse, 18 cycles

The PS&T team evaluated many options for conducting the testing, however due to its size, the shock testing proved very difficult to actually test. The amount of force to create the required shock loads was significant with the test setup weighing close to 1500lbs. After multiple discussions, it was determined that it was not possible to test a complete sine wave. Two options were available. The first option was a Shock Response Spectrum (SRS) pulse that required a ramp up and ramp down sequence. This option puts extra load into the system, which could cause a premature opening of

the EA. As an alternative, a pulse was developed with 18 positive half-sine pulses followed by 18 negative half-sine pulses. Since the floor EAs are designed to be loaded in tension and not compression, this option would be the best method to test the EA design. Figure 24 shows the pulse used, this was reversed to obtain the negative sine pulse.

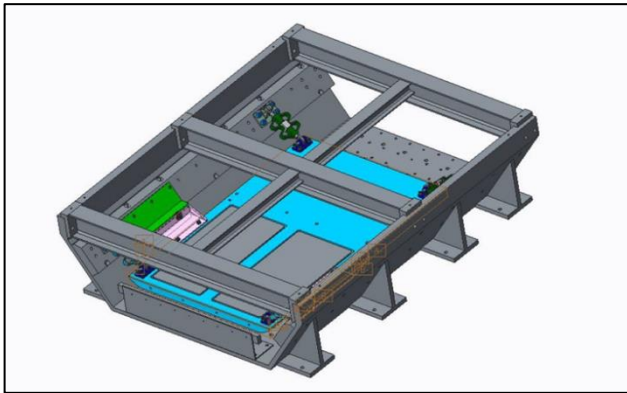


Figure 23: Flooring fixture (crew shown installed).

For this testing, a pass/fail criteria was defined. In order for the test to be considered a pass, the floor would need to be able to function as designed for a blast event after the durability test had concluded. This is evaluated by ensuring the walking floor was not bound up at the transverse bushings and that the tensile screws did not disconnect under normal loads.

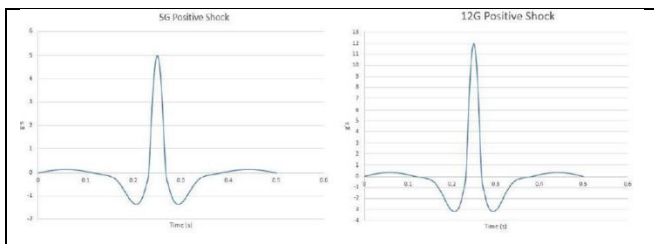


Figure 24: Adjusted road shock pulses.

16. TEST ARTICLE FABRICATION

For this test series, three floors of each configuration were fabricated. Each part was fabricated to the drawing package and then all parts were assembled at CCDC-GVSC. The floors were

partially assembled and then shipped to PS&T for installation into the test fixture. Figure 25 shows the assembled floors.



Figure 25: Assembled floors.

17. DURABILITY TESTING

The durability testing for both floors was conducted by CCDC-GVSC's PS&T group. The shock testing was conducted by Dayton T. Brown Testing facility under the supervision of PS&T engineers. For all of the testing, accelerometers were mounted to the test fixture and floor to ensure the input and response matched the expected profiles. An instrumented rod end was placed on the top end of each EA to measure the axial load imparted into the EA. The load was monitored the entire duration of the test to make sure it did not exceed the design criteria for the EAs.

Ballast weights were used to simulate the weight of the occupant's legs for the squad and the weight of the full occupants for the crew to properly load the floor. The ballast used for this testing was a wood box filled with sand bags that were rigidly attached to the floor using tie down straps and mounting bolts. For the squad configuration, 70lbs at each occupant location was used to simulate the weight of the legs on the floor. There are four occupant locations for the squad configuration. A weight of 330lbs was used to simulate the occupant weight for the crew configuration. This is distributed with 70lbs of weight directly over blast mat locations and 260lbs mounted directly over the crew seat mounting locations.

A drive file was required to be developed for each test. This is based on the 3000-mile load case

specified in the requirements for the specific mission profile. The profile is then correlated to actual road data. This data is then used to develop that actual drive file based on expected damage. Table 3 shows the drive file summary based on each road course.

Table 3: Drive file summary.

Course	Retained Bandwidth	Baseline Repeats per OMS-MP	Repeats Performed Severity Editing
PTA Paved (Perryman Paved)	1-100 hz	305	700
PTA-A (Perryman A) (PA)	1-100 hz	162	7
PTA-2 Perryman 2 (P2)	1-100 hz	447	1250
PTA-3 Perryman 3 (P3)	1-100 hz	516	5
Edited Test Duration (hr)		93.5	145
% Damage Retained 0-100hz		25.1-447.1% Average Vertical 218.5%	57.8-141.6% Average Vertical 92.3% with Leads Considered

After the drive file development, the floors were verified to be level and the instrumented rods ends were zeroed. Figure 26 shows a front view of the squad setup with the EA and Accelerometer locations. The test was ran for a total of 145 hours. The test setup was inspected at the beginning and end of each shift and every 4 hours during the run time.

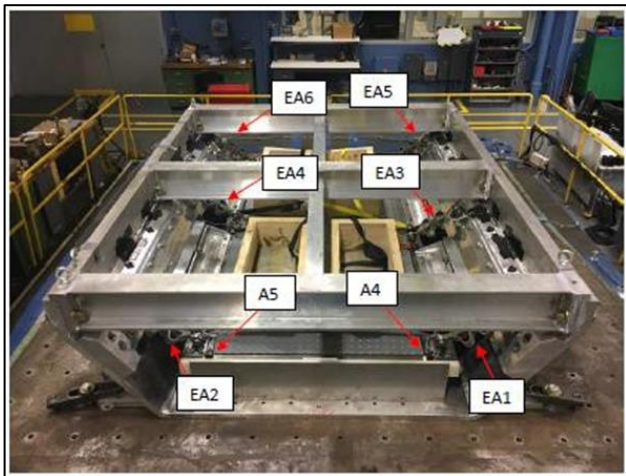


Figure 26: Test setup for road load durability (squad configuration shown).

All shock durability testing was conducted at Dayton T Brown. The testing was conducted using a T- 5500 electrodynamic shaker. The T-5500 is a

single axis shaker. Figure 27 shows the test article in the vertical and horizontal positions.



Figure 27: Electrodynamic shaker in vertical (top) and horizontal (bottom) configurations.

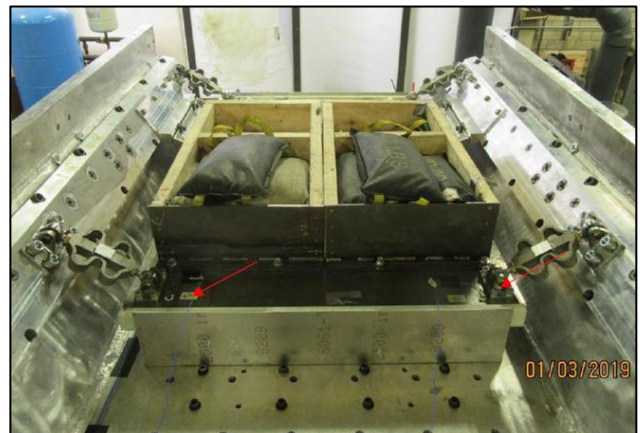


Figure 28: Test setup for road shock (crew configuration shown).

A floor fore/aft retainer was bolted to the fixture for each test. This is in place to simulate the floors mounted in a vehicle with the front and rear of the hull retaining the fore/aft movement of the floor. Figure 28 shows the crew floor with the ballast weight attached and the fore/aft retainer. Between each pulse, the floor was inspected for failures. The squad floor was tested in all three directions using the same test article. This was done to test overall shock load capability rather than a separate article for each test.

18. DURABILITY TEST RESULTS

After each test was completed, the floors were disassembled and removed from the fixture. They were then further disassembled to specifically look at the transverse plate bushing and the tensile screws.

Wear is expected on the transverse plate bushings; however, cracks and broken parts of the bushing would raise concern. Figure 29 shows an example of the transverse plate bushings after the test. The black coloring is from the lubrication that is placed on the bushings during installation. Each of the EA links were disassembled and the tensile screw assemblies were visually inspected along with the rod ends. Figure 30 shows an EA that has been disassembled. The tensile screw assembly was then inspected further to see if the tensile screw had broken or if the assembly had separated.

The squad floors showed no major issues in both the road load durability and the shock load durability tests. The rod ends did show some signs of wear on the inner race where it had been resting against the shoulder bolt. The rod end still fit tightly against the shoulder bolt and the observed condition is considered to be normal wear and tear. Figure 31 shows the rod end, the black coloring is from the lubricant used to reduce friction and wear on the rod end and shoulder bolt. The tensile screw assembly was inspected and showed no signs of separation or rotation. Figure 32 shows a squad

tensile screw assembly with the rotation mark lined up.



Figure 29: Post-test inspection of transverse panel bushing in good condition.



Figure 30: Post-test inspection of EA link assembly.



Figure 31: Post-test inspection of rod end in good condition.

The crew floor did not show any major issues during both the road load durability and the shock load durability tests. There were no failures of any kind. Again the rod ends were inspected for wear, the bushings for cracking, and the tensile screw assembly for separation.



Figure 32: Post-test inspection of tensile screw assembly.

19. System Level Durability and Live fire Testing

After the successful testing of the fully integrated floor design, two additional system level test series were conducted.

The first system level test included a representative lower hull with underbody, floor technology, and seats. This system was then sent through the same 3000 mile durability course. The goal of this test is to look at the system interaction to make sure that as a system there are not issues with the design or interferences that may not have

been previously identified. During this testing both the crew and squad configurations were tested with appropriate ballast for the occupants. Both floors performed the same as the previous tests, providing additional confidence in the system.

The second system level test series was a live fire blast test of the integrated system. This included a complete hull system mounted in the Reconfigurable asset test fixture with integrated floor, seats, and an Active Blast Mitigation System. Injury data was recorded during all of the tests in this series. The floor technology performed as designed by stroking and absorbing the blast load. The results of these tests were positive.

20. CONCLUSIONS

The crew and squad configurations successfully completed testing. They did not show any issues beyond normal wear and tear, which is expected for the 3,000-mile durability courses. The tensile screw did not fracture during any of the testing for either crew or squad floor configurations. The bushings did not show any failures and did a very good job retaining the floor both fore/aft and laterally.

This flooring system performed positively throughout both component, sub-system, and full scale system level verification testing both from a durability and survivability perspective.